



## Electromagnetic characterization of microwave sintered $\text{Sr}_{1-x}\text{Ca}_x\text{MnO}_3$ ( $0.0 \leq x \leq 0.4$ ) thick films

Rani P. Pawar, Ninad B. Velhal, Vijaya R. Puri\*

*Thick and Thin Film Device Lab, Department of Physics, Shivaji University, Kolhapur 416004, India*

Received 14 December 2012; received in revised form 21 January 2013; accepted 4 February 2013

### Abstract

*Electromagnetic characteristics of microwave sintered strontium calcium manganites thick film with variation in calcium content have been investigated. The X-ray diffraction analysis reveals tetragonal perovskite structure for all the compositions. The grain size increases with the increase in calcium content. The microwave absorption, complex permittivity, permeability and conductivity are reported in the frequency range of 8.2–18 GHz. The absorption loss is larger in Ku band while insertion loss is larger in X band. The permittivity, permeability and microwave conductivity decreases from X-band to Ku-band. The almost identical values of real part of permittivity and permeability indicate possible application as materials for impedance matching.*

**Keywords:** *manganites thick films, microwave absorption, dielectric and magnetic properties*

### I. Introduction

The methods for material property characterizations at microwave frequencies are based on transmission lines and the resonant structures developed from transmission lines [1]. With the development of radar, microwave communication technology and especially the need for antielectromagnetic interference coatings, self-concealing technology and microwave darkrooms the study of electromagnetic wave absorbing materials has increased in recent years [2–4]. The permittivity and permeability are very important properties of any medium, which describe how the electromagnetic waves propagate through that medium. Broadband electromagnetic device applications make it essential to measure the complex permittivity and permeability of materials over a wide range of frequencies. There are many ways to measure the complex permittivity of the sample, such as time and frequency domain reflection and transmission method, guided wave method, impedance method etc. [5].

Emerging trends in material synthesis indicate that rapid synthetic routes are becoming increasingly important to realize new compositions and metastable phases and materials with distinct particulate properties [6]. Conventional co-precipitation method is a dif-

fusion controlled process involving counter diffusion of the cations through the product layer. This diffusion process is controlled by an energy barrier and can be represented as  $D = D_0 \cdot e^{-AG/RT}$ . To overcome this energy barrier a relatively high thermal energy ( $>1000$  °C) is normally required, which however leads to long processing time. This kinetic and thermodynamic barrier encountered can thus be overcome by initiating in-situ exothermic reactions often achieved through wet-chemical means [7] along with microwave sintering. The microwave heating has advantages due to the enhanced diffusion processes, reduced energy consumption, very rapid heating rates and considerably reduced processing times, decreased sintering temperatures, improved physical and mechanical properties, simplicity, unique properties and lower environmental hazards.

Thick film technology has proved to be a cost-effective method highly conducive to planarization and useful for miniaturized high-frequency components. Although the concept of thick film structures is quite attractive, they are not very widely used.

In this paper, the high-frequency (8.2–18 GHz) insertion loss, absorption loss, permittivity and permeability of  $\text{Sr}_{1-x}\text{Ca}_x\text{MnO}_3$  thick film is reported. The permittivity and permeability have been measured by using voltage standing wave ratio (VSWR) method [8]. To the author's knowledge, the permittivity and permeability

\* Corresponding author: tel: +91 0231 2609230  
e-mail: vijayapuri1@gmail.com

of  $\text{Sr}_{1-x}\text{Ca}_x\text{MnO}_3$  thick film using VSWR technique in the frequency range 8.2–18 GHz are reported for the first time. All the studies have been undertaken in the absence of external magnetic field.

## II. Experimental

$\text{Sr}_{1-x}\text{Ca}_x\text{MnO}_3$  powders were prepared by chemical co-precipitation method using strontium nitrate, calcium nitrate, manganese nitrate and oxalic acid as starting materials. A solution of strontium, manganese and calcium nitrates, with concentration of 0.5 M, was prepared and added drop wise to 2 M hot (750 °C) oxalic acid solution with constant stirring. The chemicals were weighed according to required stoichiometric proportion by varying calcium content,  $x = 0.0, 0.2, 0.4$ . After cooling to room temperature the precipitate was filtered, washed with distilled water and dried. The prepared powder was sintered at 900 W for 5 h in microwave oven (model CE104VD, output power adjustable, 2450 MHz). Thick film paste of  $\text{Sr}_{1-x}\text{Ca}_x\text{MnO}_3$  was prepared by mixing the manganite powder (84 wt.%) with organic vehicle and  $\text{Bi}_2\text{O}_3$  (8 wt.%) and an inorganic binder (8 wt.%). The manganite pastes were then screen printed on the alumina substrate, dried and then fired in a microwave oven for 10 min at 300 W. The thickness of the prepared thick films was  $\sim 30 \mu\text{m}$ , measured by gravimetric method. The  $\text{Sr}_{1-x}\text{Ca}_x\text{MnO}_3$  thick films were characterized by X-ray diffraction, XRD, using Cr-K $\alpha$  radiation, ( $\lambda = 2.2890 \text{ \AA}$ ) (Philips Diffractometer PW3710) and scanning electron microscopy, SEM (JSM-6360 JEOL, Japan).

The transmission and reflection of  $\text{Sr}_{1-x}\text{Ca}_x\text{MnO}_3$  ( $0.0 \leq x \leq 0.4$ ) thick films were measured by the rectan-

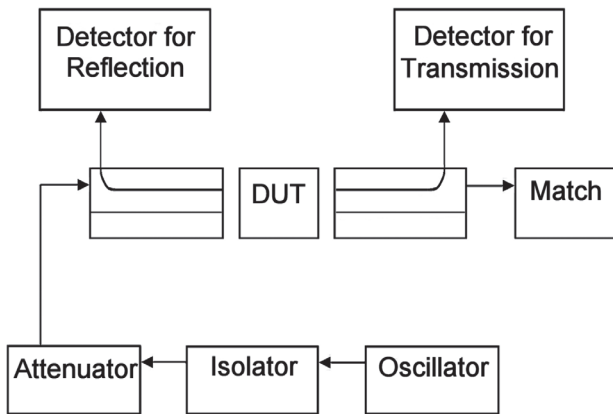


Figure 1. Schematic of microwave reflectometer setup for transmission and reflection of  $\text{Sr}_{1-x}\text{Ca}_x\text{MnO}_3$  thick film

gular waveguide reflectometer set up shown in Fig. 1. Transmission of microwaves due to thick film was measured point by point using transmission/reflection method with rectangular waveguide, consisting of the X- and Ku-band generator, isolator, attenuator, directional coupler and RF detector. The system was calibrated by measuring the output with and without the device under test (DUT). The microwave insertion loss (INL) of  $\text{Sr}_{1-x}\text{Ca}_x\text{MnO}_3$  thick films was calculated from transmission coefficient of the sample using the formula:

$$INL = -20 \log \frac{V_T}{V_I} \quad (1)$$

where,  $V_T$  is transmitted output power by thick film, and  $V_I$  is the incident power on thick film.

## III. Results and discussion

The X-ray diffraction technique was used to confirm the presence of crystalline phases and to study the influence of atmosphere on the calcinations process. The thick films have tetragonal perovskite structure with the preferred texture along (310). A typical XRD pattern of composition  $\text{Sr}_{1-x}\text{Ca}_x\text{MnO}_3$  with space group of  $I4/mcm$  is shown in Fig. 2. From the figure it is observed that as calcium concentration increases the intensity of all the peaks increases except 101 peak which decreases. This suggests that increasing the content of Ca at the Sr site progressively removes the crystal distortion. The lattice

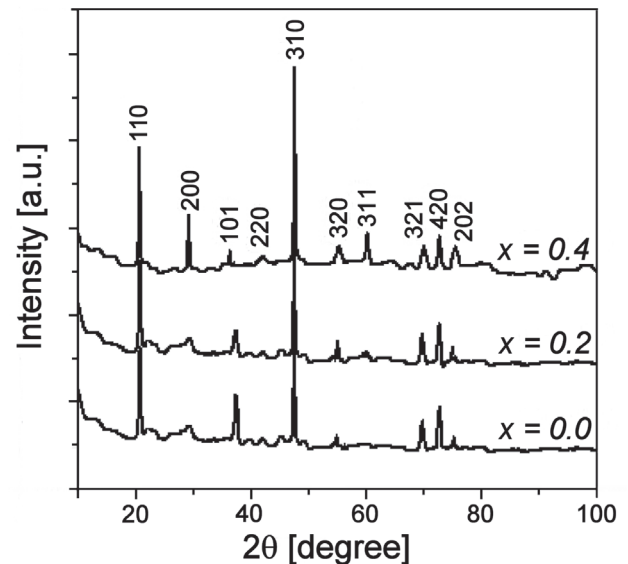


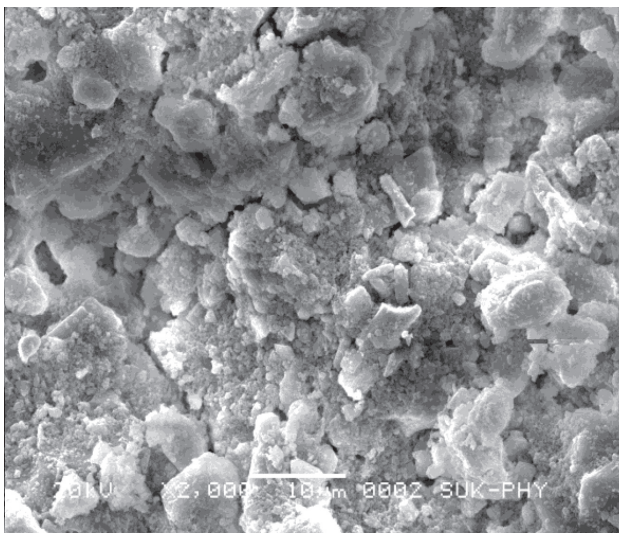
Figure 2. X-ray diffraction pattern of  $\text{Sr}_{1-x}\text{Ca}_x\text{MnO}_3$  ( $0.0 \leq x \leq 0.4$ ) thick film

Table 1. Lattice parameter, cell volume and actual density of  $\text{Sr}_{1-x}\text{Ca}_x\text{MnO}_3$  ( $0.0 \leq x \leq 0.4$ ) thick film ceramic

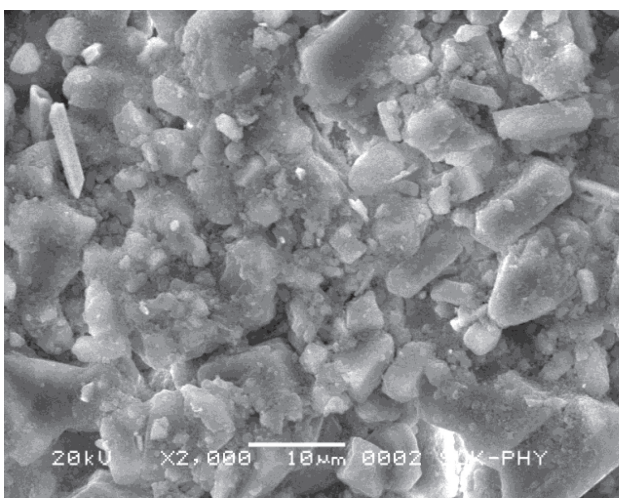
Composition, $x$	Lattice Parameter			Cell Volume [ $\text{\AA}^3$ ]	Actual Density [ $\text{g/cm}^3$ ]
	$a$ [ $\text{\AA}$ ]	$b$ [ $\text{\AA}$ ]	$c$ [ $\text{\AA}$ ]		
0.0	8.6127	8.6127	3.8102	282.64	3.45
0.2	8.5924	8.5924	3.8075	281.10	3.82
0.4	8.5748	8.5748	3.7941	278.96	4.55



a)



b)



c)

**Figure 3. Scanning electron microscope images of  $\text{Sr}_{1-x}\text{Ca}_x\text{MnO}_3$  thick films: a)  $x = 0.0$ , b)  $x = 0.2$  and c)  $x = 0.4$**

parameter and unit cell volume of the compounds decrease with calcium content (Table 1). The reason might be that the radius of  $\text{Ca}^{2+}$  is smaller than  $\text{Sr}^{2+}$ , indicating that the lattice shrinks and unit cell becomes smaller with increasing calcium concentration. This can be correlated with increase in  $\text{Mn}^{4+}$  content with doping, which has smaller size ( $0.53 \text{ \AA}$ ) than the  $\text{Mn}^{3+}$  ion ( $0.645 \text{ \AA}$ ).

The actual density ( $\rho$ ) was calculated using the formula:

$$\rho_s = \frac{m}{\pi \cdot r^2 \cdot h} \quad (2)$$

where  $m$  is the mass of the film,  $\pi r^2$  is the surface of the film and  $h$  is the thickness of the film. The change of the calculated density with calcium concentration is shown in Table 1. The density increased linearly with increase in Ca concentration from  $3.45 \text{ g/cm}^3$  to  $4.55 \text{ g/cm}^3$ . This increase may be attributed to: i) increase of rate of cation inter dispersion due to  $\text{Ca}^{2+}$  ions and ii) the increase in the reactivity of the fine manganite grains which combine to form bigger grains leading to pore reduction and volume contraction.

Figure 3 shows the scanning electron micrographs of the  $\text{Sr}_{1-x}\text{Ca}_x\text{MnO}_3$  ( $0.0 \leq x \leq 0.4$ ) thick film, and it can be observed that as calcium concentration increases grain size increases. Initially for  $x = 0.0$  spherical shaped fine grains of size  $40 \text{ nm}$  along with stacked flakes are observed, but due to increase in the calcium concentration these flakes start to coalesce and arranging themselves in flower like morphology. For  $x = 0.4$  all these grains become compact and forming tabular structure of width  $400 \text{ nm}$ . This may be due to higher atomic mobility of  $\text{Ca}^{2+}$  ions induced by liquid phase sintering.

Figure 4 shows the insertion loss as well as absorption loss of the  $\text{Sr}_{1-x}\text{Ca}_x\text{MnO}_3$  thick films in the frequency range  $8.2 \text{ GHz}$  to  $18 \text{ GHz}$ . From the figure it can be seen that in the frequency range  $8.2 \text{ GHz}$  to  $18 \text{ GHz}$  composition dependent variations are more pronounced in insertion loss than in the absorption loss. The composition with  $x = 0.0$  shows the minimal absorption loss. Insertion loss measures the energy absorbed by the transmission line in the direction of the signal path. Insertion loss is a combination of multiple sources of loss, which include: dielectric loss (related to loss tangent), connector losses and impedance mismatches (reflections), conductor losses and radiation losses. Minimum in absorption loss means that material is more microwave absorbing. At  $9.7 \text{ GHz}$  the insertion loss has maximum of  $\sim 22 \text{ dB}$  indicating that the  $\text{Sr}_{1-x}\text{Ca}_x\text{MnO}_3$  ( $0.0 \leq x \leq 0.4$ ) thick film is less transmitting and more absorbing (absorption loss is minimal). Between  $13.5$  to  $16.2 \text{ GHz}$  the absorption loss becomes high again. At  $\sim 17.2 \text{ GHz}$  the absorption loss becomes maximal whereas the insertion loss has minimal value. It means that strontium calcium manganite shows high transmittance. Absorption is the heat loss under the action be-

tween electric dipole or magnetic dipole in material and the electromagnetic field.

Usually, the microwave absorbing properties of the manganites are dominated by the magnetic and dielectric losses [9]. In order to know the parameter that dominates the absorption of these oxides, the complex dielectric permittivity  $\epsilon$  ( $\epsilon' - i\epsilon''$ ) and magnetic permeability  $\mu$  ( $\mu' - i\mu''$ ) were examined. The frequency dependence of the dielectric and magnetic absorption losses,  $\tan \delta_\epsilon = (\epsilon''/\epsilon')$  and  $\tan \delta_\mu = (\mu''/\mu')$ , were also calculated. From the position of the voltage standing wave minimum and using the Smith chart [10] the real and imaginary permittivity were obtained. The Smith chart was used to find the phase change due to the manganite material in the path of microwaves.

Permittivity and permeability of strontium calcium manganite can be determined using the VSWR measurement set up. The VSWR measurement setup was almost the same as the waveguide reflectometer setup; instead of two 3 dB directional couplers VSWR slotted section was used. Initially the slotted section was calibrated with air and alumina. The alumina and manganite thick films acts as a load to the transmission of the microwaves and microwaves reflected back from that load. The positions of the minimum of the standing wave were compared with that of air. As impedance is mismatched, the position of the minimum is shifted by placing the thick films as load. The reflection coefficient was also measured. The Smith chart was used to find the phase change due to the  $\text{Sr}_{1-x}\text{Ca}_x\text{MnO}_3$  ( $0.0 \leq x \leq 0.4$ ) thick film in the path of microwaves and permittivity measured by using the formula [11]:

$$\epsilon' = \left( 1 + \frac{\Delta\phi \cdot \lambda_0}{360 \cdot d} \right)^2 \quad (3)$$

$$\epsilon'' = \left( \frac{\Delta\phi \cdot \lambda_0 \sqrt{\epsilon'}}{8.686 \cdot \pi \cdot d} \right)^2 \quad (4)$$

where  $\Delta\phi$  is phase difference between incident and reflected waves,  $\lambda_0$  is guided wavelength and  $d$  is thickness of the sample.

From Fig. 5 it is observed that  $\epsilon'$  values are almost constant between 11 to 18 GHz but they increase slightly for frequencies below 11 GHz which suggest that the most probable mechanism in this frequency range is orientational polarization [12]. Composition dependent variations are also observed it means that as calcium content increases in strontium manganite real part of permittivity decreases. For  $x = 0.0$  the value of  $\epsilon'$  is 12.6 but for  $x = 0.4$  it decreases to  $\sim 10.2$  this may be attributed to decrease in mobility of charge carrier with increase in calcium concentration. In case of the dielectric loss ( $\epsilon''$ ) as frequency increases in the 8.2–18 GHz range loss decreases from 0.23 and becomes minimal of about 0.01 at 18 GHz. Below 12 GHz the thick films of all compositions show larger loss. The absorption data also show similar frequency dependent effects.

The real and imaginary permeability of the calcium strontium manganite thick film is shown in Fig. 6. The permeability of the  $\text{Sr}_{1-x}\text{Ca}_x\text{MnO}_3$  thick films were calculated from the reflectance using formula [13]:

$$\mu' = \frac{1 + 2\Gamma + \Gamma^2}{1 - 2\Gamma + \Gamma^2} \times \epsilon' \times C \quad (5)$$

$$\mu'' = \frac{1 + 2\Gamma + \Gamma^2}{1 - 2\Gamma + \Gamma^2} \times \epsilon'' + C \quad (6)$$

where  $G$  is reflectance in dB and  $C$  is standardizing coefficient obtained from standard sample. From Fig. 6 it is observed that in the low-frequency region the strontium calcium manganite shows the larger  $\mu'$  value, but in the high-frequency region,  $\mu'$  values are almost the same. The demagnetizing field generated by the magnetic poles on the surface of magnetic fillers plays a very important and characteristic role in the permeability of material [14]. Both  $\mu'$  and  $\mu''$  show a decreasing

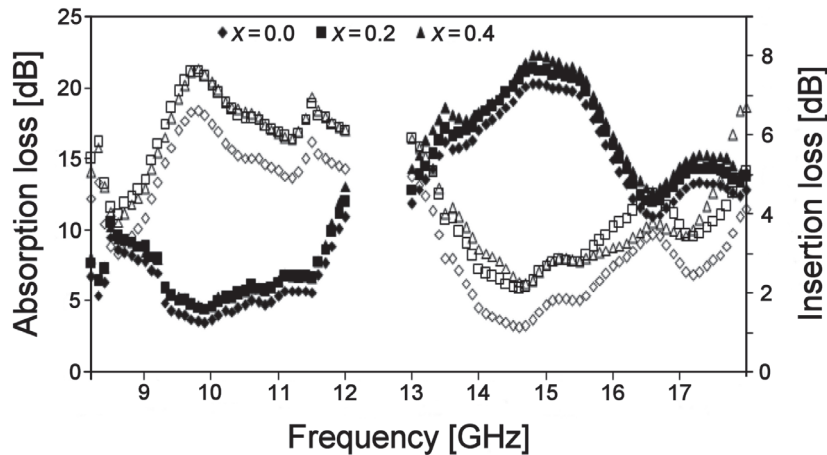


Figure 4. Effect of calcium on microwave absorption loss and insertion loss. Dark symbols represent the absorption loss while unfilled symbols represent the insertion loss.

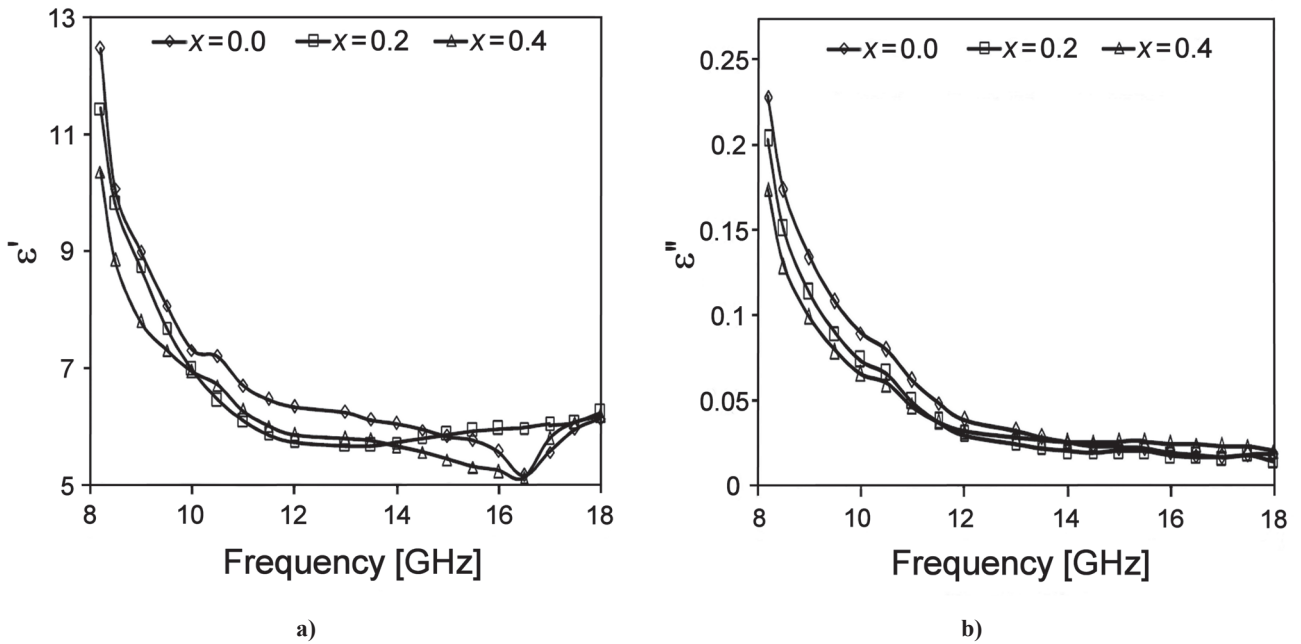


Figure 5. Variation of real and imaginary part of permittivity of Sr<sub>1-x</sub>Ca<sub>x</sub>MnO<sub>3</sub> (0.0 ≤ x ≤ 0.4) thick film with frequency

trend with increasing frequency, due to the lower resonance frequency range of the strontium calcium manganite powder than the measured frequency range (8.2–18 GHz) [15]. The enhanced  $\mu'$  and  $\mu''$  values will improve the microwave absorbing effect by transferring electromagnetic energy into heat energy [16].

The electromagnetic loss mechanism of the materials can be explained by the characteristic change of loss tangent (loss factor) for Sr<sub>1-x</sub>Ca<sub>x</sub>MnO<sub>3</sub> (0.0 ≤ x ≤ 0.4). According to the data of electromagnetic parameters (complex permittivity and complex permeability), the relations between the dielectric loss tangent ( $\tan \delta_\epsilon$ ) and magnetic loss tangent ( $\tan \delta_\mu$ ) and microwave frequency for the samples have been calculated, as shown Fig. 7.

In the whole range of frequency, the value of  $\tan \delta_\epsilon$  is similar to  $\tan \delta_\mu$ . The frequency dependent dielectric loss is more prominent in the X-band than in the Ku-band, whereas the frequency dependent magnetic loss

decreases linearly up to 18 GHz. Magnetic losses are caused by the time lag of the magnetization vector  $M$  behind the magnetic field vector  $H$  [9]. The change of the magnetization vector is generally brought about by rotation of the magnetization or the domain wall displacement. These motions lag behind the change of the magnetic field and contribute to  $\mu''$ . The smaller the particle size, the weaker the spins coupling at the surface of the particle, which makes the magnetic relaxation behaviour more complex, and will give rise to a magnetic loss mechanism.

The microwave conductivity of the Sr<sub>1-x</sub>Ca<sub>x</sub>MnO<sub>3</sub> (0.0 ≤ x ≤ 0.4) thick films was calculated using the formula [17]:

$$\sigma = \omega \cdot \epsilon_0 \cdot \epsilon'' \quad (7)$$

where  $\omega$  is angular frequency,  $\epsilon_0$  is permittivity of free space and  $\epsilon''$  is dielectric loss of material.

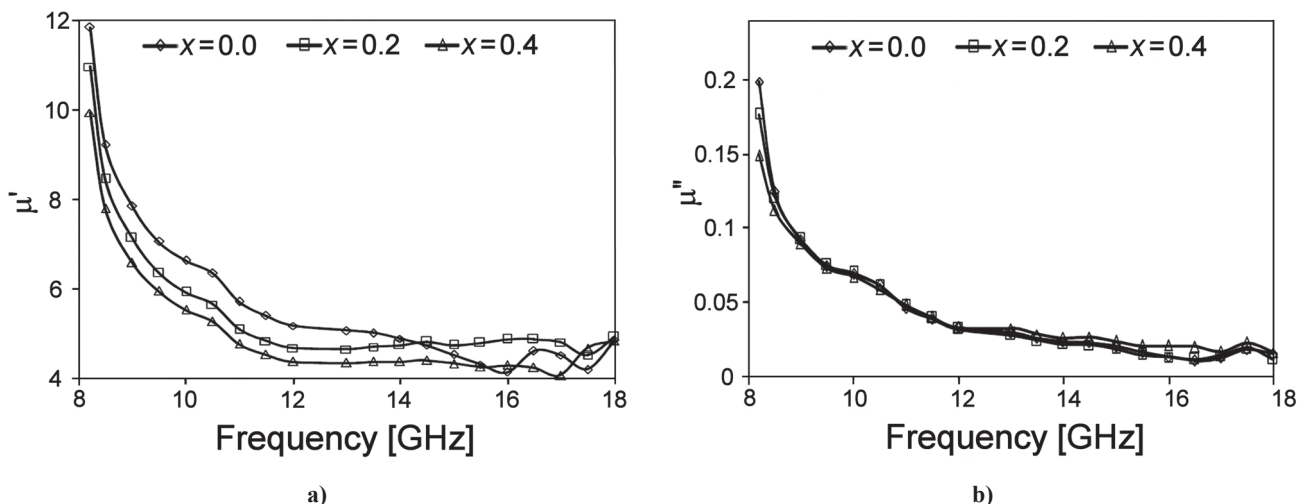


Figure 6. Frequency dependent real and imaginary part of permeability of Sr<sub>1-x</sub>Ca<sub>x</sub>MnO<sub>3</sub> (0.0 ≤ x ≤ 0.4) thick film

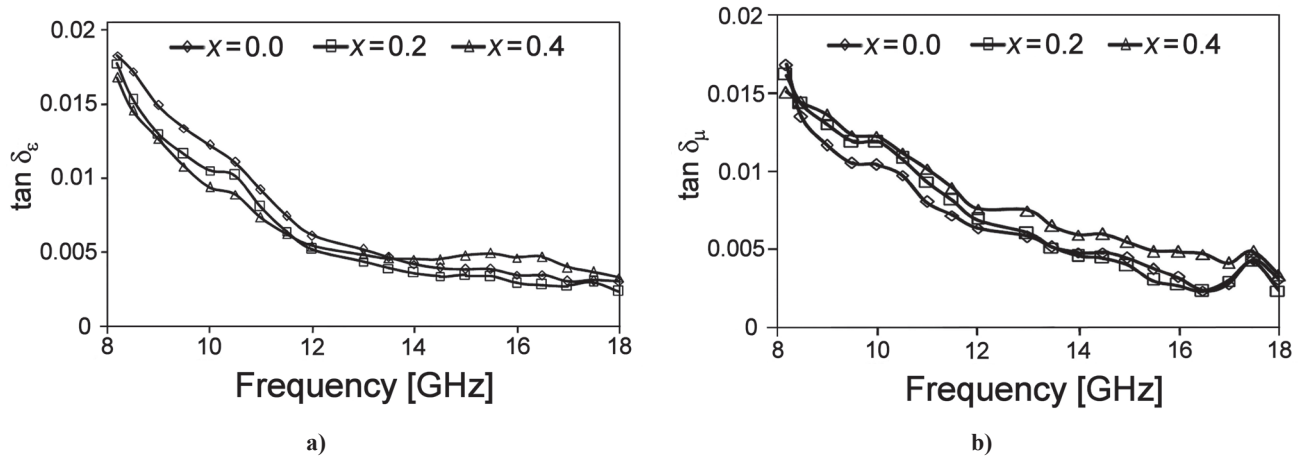
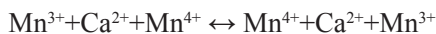
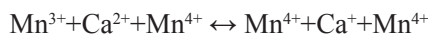


Figure 7. The dielectric and magnetic losses,  $\tan \delta_\epsilon$  and  $\tan \delta_\mu$ , as a function of frequency for  $x = 0.0, 0.2, 0.4$

From Fig. 8, it is observed that as calcium content increases microwave conductivity decreases. The conductivity varies from  $\sim 0.1$  S/cm for the composition  $x = 0$ ,  $\sim 0.09$  S/cm for  $x = 0.2$  and  $>0.08$  S/cm for  $x = 0.4$ . As calcium content increases the frequency dependent variations are decreased. Conduction is caused by the hopping of electrons between the Mn<sup>3+</sup> and Mn<sup>4+</sup>. In other words it can be described with:



This means that both Mn and Ca cations act as hopping ions which causes the decrease in the conductivity.

To the authors knowledge there are no reports available on the microwave conductivity of Sr<sub>1-x</sub>Ca<sub>x</sub>MnO<sub>3</sub> thick film in the 8.2–18 GHz frequency range.

#### IV. Conclusions

The Sr<sub>1-x</sub>Ca<sub>x</sub>MnO<sub>3</sub> thick films, synthesized by chemical co-precipitation method and deposited by screen printing, show absorbing nature over a large range of frequency in the X-band (minimum absorp-

tion loss) whereas transmitting nature in the Ku-band region (minimum insertion loss) of the electromagnetic spectrum. Densification could be achieved by microwave sintering technique with low sintering temperature and reduced soaking time, which results in low emission of nitrates and hence the process is environmentally friendly. Uniform and fine grains as well as flakes and tabular structure were observed as a result of calcium doping. The investigation of complex dielectric permittivity and magnetic permeability indicates that the absorption can be ascribed to the magnetic and dielectric losses. The microwave permittivity of the Sr<sub>1-x</sub>Ca<sub>x</sub>MnO<sub>3</sub> ( $0.0 \leq x \leq 0.4$ ) thick films decreases with increase in calcium concentration. The microwave conductivity also decreases with the increase in calcium content. Both permittivity as well as permeability matches with each other, i.e.  $\epsilon^* = \mu^*$  indicating that the strontium calcium manganite can be used as an impedance matched material. The unique properties of the doped manganese oxides provide an important foundation for developing the materials with strong microwave absorption in certain band as well as high transmittance in certain bands resulting in wide application prospects.

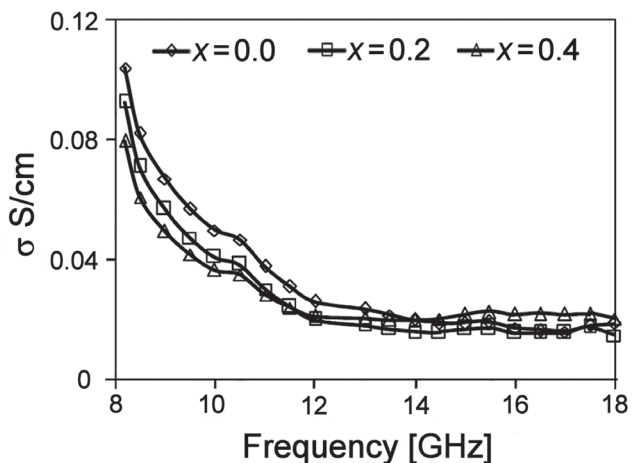


Figure 8. Frequency dependent variations in microwave conductivity of Sr<sub>1-x</sub>Ca<sub>x</sub>MnO<sub>3</sub> thick film

**Acknowledgements:** One of the authors Vijaya Puri would like to thank the UGC India for Award of Research Scientist ‘C’. R.P. Pawar would like to thank the DST PURSE scheme for their financial support. All authors acknowledge the UGC-SAP and DST-FIST.

#### References

1. S. Borah, N.S. Bhattacharyya, “Broadband measurement of complex permittivity of composite at microwave frequencies using scalar scattering parameters”, *Prog. Elect. Resear. M.*, **13** (2010) 53–68.
2. H.S. Cho, S.S. Kim, “M-exaferrites with planar magnetic anisotropy and their application to high-frequency microwave absorbers”, *IEEE Trans. Magn.*, **35** (1999) 3151–3153.

3. S.P. Ruan, B.K. Xu, H. Suo, F.Q. Wu, S.Q. Xiang, M.Y. Zhao, "Microwave absorptive behavior of ZnCo-substituted W-type Ba hexaferrite nano crystalline composite material", *J. Magn. Magn. Mater.*, **212** (2000) 175–177.
4. M.R. Anantharaman, S. Sindhu, S. Jagatheesan, K.A. Malini, P. Kurian, "Dielectric properties of rubber ferrite composites containing mixed ferrites", *J. Phys. D: Appl. Phys.*, **32** (1999) 1801–1810.
5. U.C. Hasar, "Unique permittivity determination of low-loss dielectric materials from transmission measurements at microwave frequencies", *Prog. Elect. Resear. C.*, **107** (2010) 31–46.
6. P.R. Bonneau, R.F. Jarvis, R.B. Kaner, "Rapid solid-state synthesis of materials from molybdenum disulphide to refractories", *Nature*, **349** (1991) 510–512.
7. R.K. Sahu, M.L. Rao, S.S. Manoharan, "Microwave synthesis of magneto resistive  $\text{La}_{0.7}\text{Ba}_{0.3}\text{MnO}_3$  using inorganic precursors", *J. Mater. Sci.*, **36** (2001) 4099–4102.
8. R.N. Jadhav, V. Puri, "Microwave absorption, conductivity and complex permittivity of fritless  $\text{Ni}_{(1-x)}\text{Cu}_x\text{Mn}_2\text{O}_4$  ( $0 \leq x \leq 1$ ) ceramic thick film: effect of copper", *Prog. Elect. Resear. C.*, **8** (2009) 149–160.
9. R.P. Pawar, R.N. Jadhav, V. Puri, "Effect of Ca on microwave properties of strontium mangnaite synthesized by microwave processing", *Elect. Mater. Lett.*, **8** [3] (2012) 321–324.
10. D.C. Kulkarni, U.B. Lonkar, V. Puri, "High-frequency permeability and permittivity of  $\text{Ni}_x\text{Zn}_{(1-x)}\text{Fe}_2\text{O}_4$  thick film", *J. Magn. Magn. Mater.*, **320** (2008) 1844–1848.
11. M.B. Shelar, R.N. Jadhav, V. Puri, "Microwave studies of ferrite-ferroelectric composites prepared through self propagating auto combustion route", *Prog. Elect. Resear. C.*, **17** (2010) 55–65.
12. S.S. Kim, S.T. Kim, J.M. Ahn, K.H. Kim, "Magnetic and microwave absorbing properties of Co-Fe thin films plated on hollow ceramic microspheres of low density", *J. Magn. Magn. Mater.*, **271** (2004) 39–45.
13. D.C. Kulkarni, V. Puri, "Ku band microwave studies of fritless strontium hexaferrite thick films", *Microelect. Int.*, **27** (2010) 143–147.
14. C.H. Peng, H.W. Wang, S.W. Kan, M.Z. Shen, Y.M. Wei, S.-Y. Chen, "Microwave absorbing materials using Ag-NiZn ferrite core-shell nanopowders as fillers" *J. Magn. Magn. Mater.*, **284** (2004) 113–119.
15. X.L. Dong, X.F. Zhang, H. Huang, F. Zuo, "Enhanced microwave absorption in Ni/polyaniline nanocomposites by dual dielectric relaxations", *Appl. Phys. Lett.*, **92** (2008) 013127.
16. Z. Zou, A.G. Xuan, Z.G. Yan, Y.X. Wu, N. Li, "Preparation of  $\text{Fe}_3\text{O}_4$  particles from copper/iron ore cinder and their microwave absorption properties", *Chem. Eng. Sci.*, **65** (2010) 160–164.
17. S.N. Mathad, R.N. Jadhav, R.P. Pawar, V. Puri, "Dielectric spectroscopy and microwave conductivity of bismuth strontium manganites at high frequencies", *Elect. Mater. Lett.*, article in press.

